CellPress

Neuron
Article

SorCS2 Regulates Dopaminergic Wiring and Is Processed into an Apoptotic Two-Chain Receptor in Peripheral Glia

Simon Glerup,[1,2,3,*] Ditte Olsen,[1,2] Christian B. Vaegter,[1,2] Camilla Gustafsen,[1,2] Susanne S. Sjoegaard,[1,2] Guido Hermey,[1,4] Mads Kjolby,[1,2] Simon Molgaard,[1,2,5] Maj Ulrichsen,[1,2] Simon Boggild,[1,2] Sune Skeldal,[1] Anja N. Fjorback,[1,2] Jens R. Nyengaard,[5] Jan Jacobsen,[6] Dirk Bender,[6] Carsten R. Bjarkam,[7] Esben S. Sørensen,[8] Ernst-Martin Füchtbauer,[8] Gregor Eichele,[9] Peder Madsen,[1] Thomas E. Willnow,[10] Claus M. Petersen,[1] and Anders Nykjaer[1,2,3,*]

[1]The Lundbeck Foundation Research Center MIND
[2]Danish Research Institute of Translational Neuroscience DANDRITE Nordic-EMBL Partnership
Department of Biomedicine, Aarhus University, Vennelyst Boulevard 4, 8000 C Aarhus, Denmark
[3]Department of Neuroscience, Mayo Clinic, Jacksonville, FL 32224, USA
[4]Center for Molecular Neurobiology, University Medical Center Hamburg-Eppendorf, 20251 Hamburg, Germany
[5]MIND Center, Stereology and Electron Microscopy Laboratory, Aarhus University, 8000 C Aarhus, Denmark
[6]PET Center
[7]Department of Neurosurgery
Aarhus University Hospital, 8000 C Aarhus, Denmark
[8]Department of Molecular Biology and Genetics, Aarhus University, 8000 Aarhus, Denmark
[9]Department of Genes and Behaviour, Max Plack Institute, 37077 Göttingen, Germany
[10]Max-Delbrueck-Center for Molecular Medicine, 13125 Berlin, Germany
*Correspondence: sg@biokemi.au.dk (S.G.), an@biokemi.au.dk (A.N.)
http://dx.doi.org/10.1016/j.neuron.2014.04.022

SUMMARY

Balancing trophic and apoptotic cues is critical for development and regeneration of neuronal circuits. Here we identify SorCS2 as a proneurotrophin (proNT) receptor, mediating both trophic and apoptotic signals in conjunction with p75^{NTR}. CNS neurons, but not glia, express SorCS2 as a single-chain protein that is essential for proBDNF-induced growth cone collapse in developing dopaminergic processes. SorCS2- or p75^{NTR}-deficient in mice caused reduced dopamine levels and metabolism and dopaminergic hyperinnervation of the frontal cortex. Accordingly, both knockout models displayed a paradoxical behavioral response to amphetamine reminiscent of ADHD. Contrary, in PNS glia, but not in neurons, proteolytic processing produced a two-chain SorCS2 isoform that mediated proNT-dependent Schwann cell apoptosis. Sciatic nerve injury triggered generation of two-chain SorCS2 in p75^{NTR}-positive dying Schwann cells, with apoptosis being profoundly attenuated in *Sorcs2*$^{-/-}$ mice. In conclusion, we have demonstrated that two-chain processing of SorCS2 enables neurons and glia to respond differently to proneurotrophins.

INTRODUCTION

During embryonic and early postnatal development, axons navigate to their targets through a process controlled by attractive and repulsive cues and signals regulating growth cone morphology. Once innervation is completed, a period of pruning follows that serves to nourish axons and neurons that made proper synaptic contacts while eliminating those that failed to do so. Many trophic cues persist during adulthood and secure neuronal integrity but apoptotic signals become dormant (Huang and Reichardt, 2003). However, following injury to the nervous system, apoptosis signaling may be reactivated, causing death of the lesioned neurons and their neighboring glia cells (Chen et al., 2007; Lee et al., 2001). The mechanisms that switch between trophic and apoptotic responses are incompletely understood, but signaling by neurotrophins and their precursors is likely to be involved (Nykjaer et al., 2005; Skeldal et al., 2011).

The neurotrophin (NT) family comprises nerve growth factor (NGF), brain-derived neurotrophic factor (BDNF), and neurotrophin-3 (NT-3) and neurotrophin-4 (NT-4; Arancio and Chao, 2007; Chao, 2003; Huang and Reichardt, 2003). Among other functions, these factors stimulate neuronal survival, differentiation, axon guidance, and synaptic strengthening by engaging members of the receptor tyrosine kinases Trks in conjunction with p75^{NTR}. NTs are commonly secreted as precursors denoted proneurotrophins (proNT). In contrast to their mature counterparts, proNTs induce apoptosis, growth cone collapse, and facilitate synaptic retraction by a mechanism that requires p75^{NTR} but is independent of Trk receptors (Lee et al., 2001; Nykjaer et al., 2004; Rösch et al., 2005; Woo et al., 2005; Yano et al., 2009). The capacity of proNTs to induce apoptosis is considered particularly important in conditions of acute and insidious neuronal and glial cell degeneration such as spinal cord and peripheral nerve injury, seizure, and aging (Arancio and Chao, 2007; Beattie et al., 2002; Ibáñez and Simi, 2012; Nykjaer et al., 2005; Petratos et al., 2003).

The Vps10p-domain (Vps10p-D) family of neuronal receptors comprises sortilin, SorLA, and SorCS1, SorCS2, and SorCS3. We previously reported that sortilin, the archetype Vps10-D receptor (Quistgaard et al., 2009), plays a central role in regulating cell fate (Jansen et al., 2007; Nykjaer et al., 2004, 2005; Nykjaer and Willnow, 2012). It is required for proNTs to induce apoptosis by forming a ternary death-inducing receptor-ligand complex with $p75^{NTR}$ and either proNGF, proBDNF, or proNT3 (Nykjaer et al., 2004; Tauris et al., 2011; Teng et al., 2005; Yano et al., 2009). Accordingly, sortilin knockout mice exhibit reduced proNGF-dependent apoptosis under conditions where neuron death normally prevails, including pruning of retinal ganglion cells, senescence of sympathetic neurons, and injury to corticospinal neurons (Jansen et al., 2007).

Surprisingly, Schwann cell (SC) apoptosis induced by sciatic nerve injury requires $p75^{NTR}$ expression (Petratos et al., 2003; Soilu-Hänninen et al., 1999; Syroid et al., 2000), yet sortilin is absent from these cells (Nykjaer et al., 2004). This observation suggested that SC death is either independent of proNTs or requires a yet unknown $p75^{NTR}$ coreceptor. Now, we establish the sortilin-related receptor SorCS2 as a proNT binding partner and coreceptor to $p75^{NTR}$ that displays a remarkably complementary cell type-specific and subcellular expression compared to sortilin. We find that SorCS2 is unique among the members of the Vps10p-D receptor family because it exists in single- and two-chain forms that engage in axonal retraction and transmission of apoptotic signals, respectively. This example shows that proteolytic processing of a receptor can regulate two disparate functions critical for balancing trophic and apoptotic signals in the nervous system.

RESULTS

Differential Expression of SorCS2 in Neurons and Glia Cells in the Central and Peripheral Nervous Systems

We first characterized SorCS2 expression in the adult murine CNS with immunohistochemistry using a polyclonal antibody against the extracellular part of SorCS2 (αECD). In the cerebellum, cortex, and hippocampus, αECD intensely stained Purkinje cells and NeuN-positive pyramidal neurons but not GFAP-positive glia cells (Figures 1A–1D). SorCS2 localization was clearly evident in neuronal processes and to a much a larger extent than the related receptor sortilin, which was mainly concentrated around the soma (Figure 1A). The opposite expression pattern for SorCS2 was observed in the peripheral nervous system (PNS). Here, SorCS2 levels were high in satellite cells of dorsal root ganglia (DRG) and in cultured glia cells of superior cervical ganglia and absent from the corresponding neurons (Figures 1E and 1F). We confirmed this divergent expression pattern with western blot (WB) analysis of cultured neurons and glia cells derived from the CNS and PNS, respectively. Robust immunoreactive bands were present in the hippocampal neurons and DRG glia, but not in cortical glia and neurons from the PNS (Figure 1G). Remarkably, while SorCS2 in hippocampal neurons mainly migrated as one distinct band, a double band of 122 and 104 kDa was present in DRG glia, with the 104 kDa band being most intense. The data suggested that SorCS2 exists in two variants that are differentially expressed in the CNS and PNS.

SorCS2 Comprises Two Fragments in PNS Glia

The nucleotide sequence of SorCS2 predicts a protein of 1,159 amino acids (aa) comprising a short propeptide of 69 residues (aa 51–119; based on homology with sortilin) followed by a Vps10p-D (aa 120–785), a polycystic kidney disease domain (aa 786–876), a leucine-rich domain (aa 877–1,078), a transmembrane spanning region (aa 1,079–1,099), and a short cytoplasmic tail of 60 aa (Figures S1A and S1B available online). When expressed in HEK293 cells, we observed three bands in WB analysis (αECD), a faint band of approximately 130 kDa in addition to the 122 kDa and 104 kDa bands seen in the DRG glia, demonstrating that the two isoforms are not produced by alternative splicing (Figure 1H). SorCS2 has seven potential N-linked glycosylation sites, but heterogeneous glycosylation did not account for the triple band as it still persisted, albeit at lower molecular weight, following PNGase-mediated deglycosylation (Figure 1I). Neither treatment with neuraminidase nor O-glycosidase changed their relative migration in the gel (data not shown). When probing with an antibody against the propeptide sequence of SorCS2 (αPRO), only the 130 kDa protein was recognized, indicating that the propeptide had been liberated from the 122 and 104 kDa isoforms that were detected by αECD (Figure 1H). An antibody against the cytoplasmic tail (αCT) detected the 130 and 122 kDa bands in addition to a band of 18 kDa, indicating the existence of a C-terminal receptor fragment (Figure 1J). The 18 kDa band was also present in DRGs but not in brain homogenates (Figure 1K).

Proteolytic Processing Generates a Two-Chain Receptor Variant

SorCS2 contains four putative cleavage sites for furin-like proprotein convertases: three sites conform to the consensus sequence RXXR and localize to the propeptide at aa 66–69 (site 1), 84–87 (site 2), and 117–119 (site 3), respectively, and one highly conserved R/KKR motif positioned at residues 1,028–1,030 (site 4) in the juxtamembrane leucine-rich repeat domain (Figures S1A–S1C). To identify the positions subject to proteolytic processing, we expressed a soluble and truncated receptor variant (SorCS2-sol) that comprises the entire extracellular domain. N-terminal sequencing revealed three distinct N termini starting at Ser^{70}, Ala^{120}, and Ser^{1031}, respectively, demonstrating that SorCS2 can be cleaved in both the first, third, and fourth consensus motifs (Figures 2A and S1A–S1C). In support of this, disruption of sites 1 and 3 at Ser^{70} and Ala^{120} by substitution of alanines for the RXXR motif (SorCS2-pro) considerably diminished propeptide processing of the full-length receptor as determined with western blotting with αECD and αCT (Figure 2B, left and middle). Disrupting the fourth consensus cleavage site at RKR (SorCS2-one) preceding Ser^{1031} and positioned 48 residues proximal to the membrane-spanning region, completely eliminated expression of the 104 kDa fragment (Figure 2B, left and middle). In the converse situation, we produced a mutant in which the Ser^{1031} cleavage site was changed from RKR to RRKR by substituting Thr^{1027} to arginine to introduce an ideal proprotein convertase cleavage site (SorCS2-two). The 104 kDa cleaved receptor was now the sole isoform recognized by αECD and no high-molecular-weight bands were detectable with αCT, suggesting immediate proteolytic

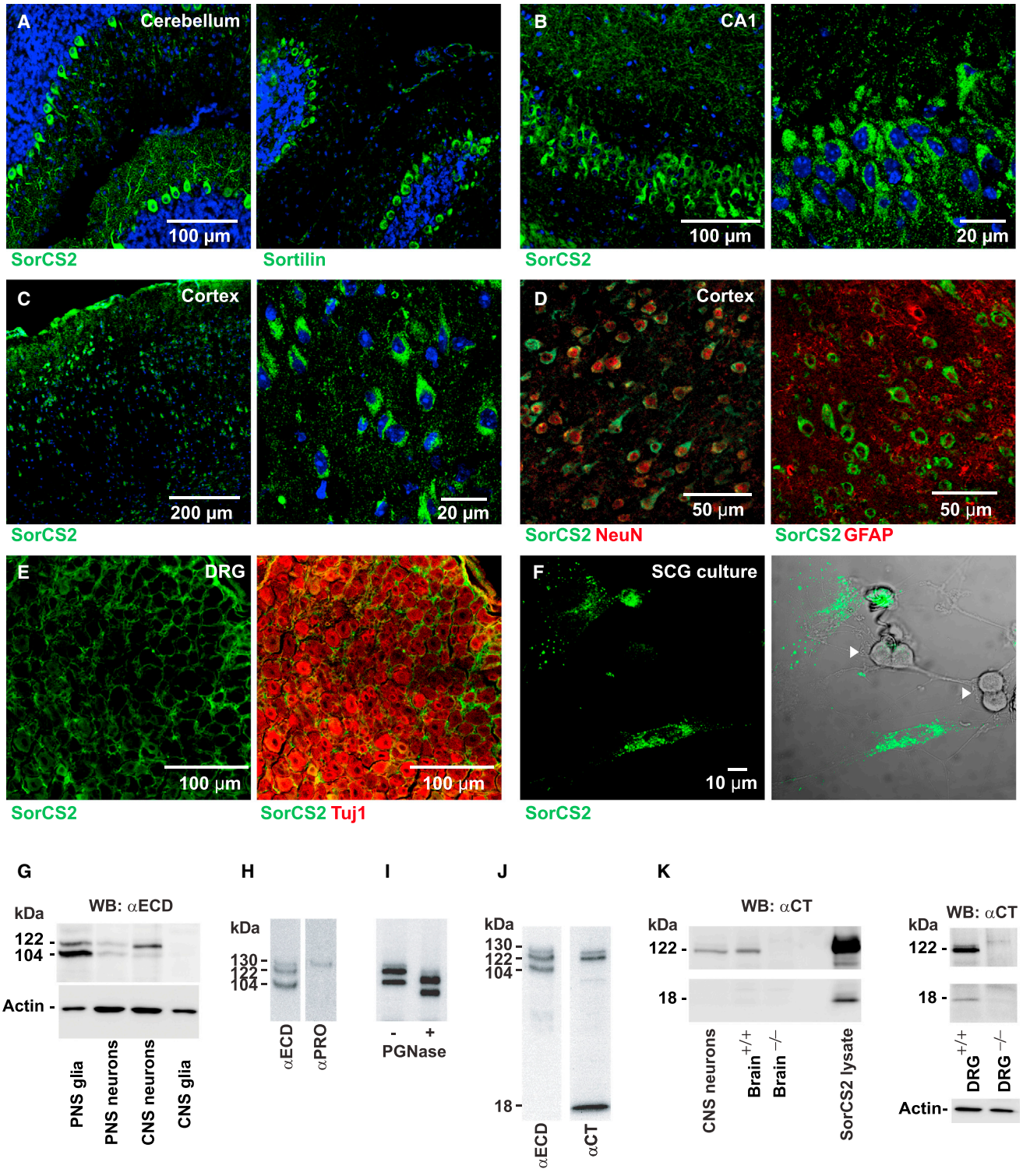

Figure 1. SorCS2 Exists in Tissue-Specific Isoforms

(A–C) Immunofluorescence microscopy for SorCS2 and sortilin in adult cerebellum and for SorCS2 in CA1 of the hippocampus and cortex (10-week-old mice). Coronal sections are shown.

(D) SorCS2 (green) is present in neurons marked by the marker NeuN (red) but not in GFAP-positive glia cells (red).

(E) In DRGs, SorCS2 (green) is seen in satellite cells but not in Tuj1-positive neurons (red).

(legend continued on next page)

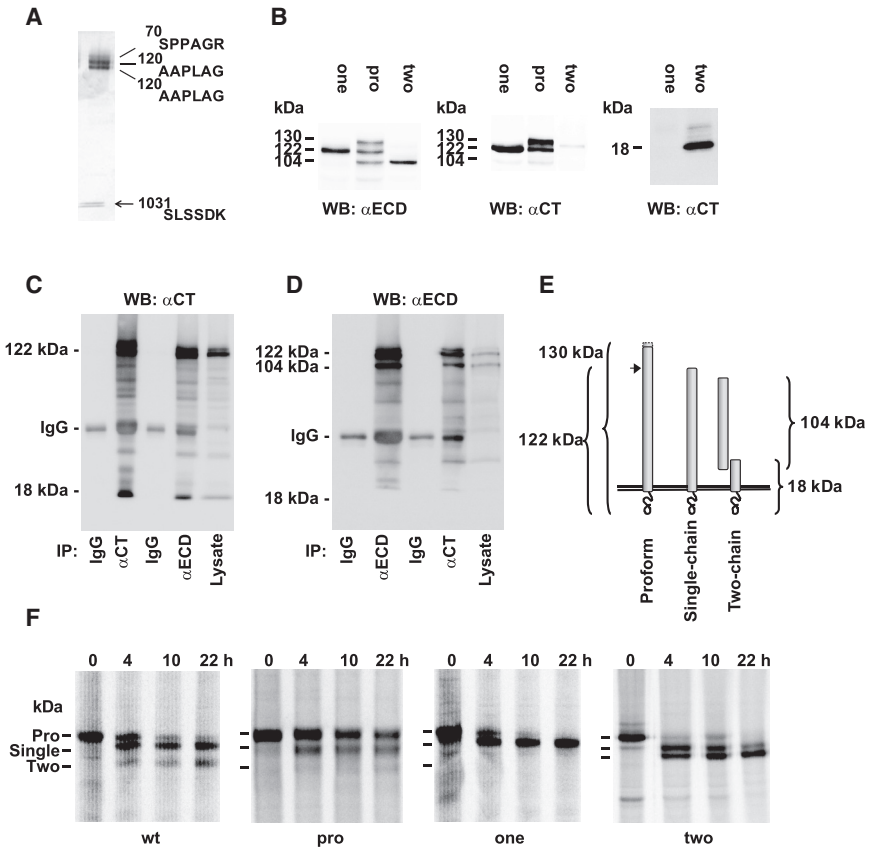

Figure 2. Single-Chain and Two-Chain SorCS2 Isoforms Are Generated Sequentially

(A) N-terminal sequencing of SorCS2-sol isoforms following purification from conditioned medium of transfected CHO cells. The first six amino acids of each isoform are indicated.

(B) αECD and αCT WB of HEK293 cells transfected with SorCS2 variants with mutated processing sites (SorCS2-one, SorCS2-pro, and SorCS2-two).

(C and D) Coimmunoprecipitation of the C-terminal fragment with the N-terminal fragment followed by WB using αCT or αECD are given. Nonimmune rabbit IgG was used as negative control for immunoprecipitation.

(E) Structure of SorCS2 variants; the ~130 kDa proform, the ~122 kDa single-chain, and the ~104 kDa two-chain receptor tethered to its ~18 kDa C-terminal fragment.

(F) HEK293 cells stably transfected with SorCS2-wt, SorCS2-pro, SorCS2-one, or SorCS2-two were pulsed for 4 hr in the presence of Brefeldin A and chased at 37°C for the indicated times. Subsequently, proteins were immunoprecipitated using αECD, and visualized using fluorography. The proform (Pro), single-chain (Single), and two-chain (Two) forms of SorCS2 are indicated.

processing of the 122 kDa single-chain receptor (Figure 2B, left and middle). In agreement, the 18 kDa peptide, which was absent from cells expressing SorCS2-one, was clearly visible in SorCS2-two (Figure 2B, right).

The combined data suggested that SorCS2 can undergo two processing events. The 130 kDa SorCS2, denoted the proform, can be cleaved immediately after its propeptide to generate a 122 kDa single-chain receptor and, second, in the extracellular domain close to the plasma membrane to produce two fragments; one of 104 kDa comprising most of the extracellular domain and one of 18 kDa encompassing the transmembrane domain and cytoplasmic tail.

We next asked whether the 104 kDa extracellular and 18 kDa C-terminal fragments of SorCS2 remain associated after processing. Indeed, both receptor fragments coimmunoprecipitated (samples not crosslinked) when using αCT or αECD antibodies; i.e., when the 18 kDa fragment was pulled down the 104 kDa band came along and vice versa (Figures 2C and 2D). This interaction was noncovalent because the 104 kDa band was also present when SorCS2 was analyzed with αECD western blotting of cell lysates in the absence of reducing agents (Figure S1D). Moreover, in cells expressing two-chain SorCS2 double-immunostaining with αCT and a monoclonal anti-ECD antibody, the extracellular domain and the cytoplasmic tail colocalized at the plasma membrane and in intracellular vesicles, indicating that the 104 kDa fragment remain associated with the plasma membrane (Figure S1E). Finally, surface biotinylation experiments further revealed that both isoforms were equally represented on the cell surface (Figure S1F), and when chased with surface-bound αECD, internalization and retrograde transport of the antibody to the trans-Golgi network was similar between the two receptor isoforms. This suggests that cellular trafficking of the 122 kDa single-chain receptor and 104 kDa

(F) Dissociated culture of superior cervical ganglia neurons and glia from P0 mice shows that SorCS2 (green) is present in glia and not neurons. Right: is a merger of immunofluorescense and differential interference contrast images. Neurons were identified based on morphology (white arrowheads).

(G) Anti-SorCS2 (αECD) western blot analyses (WB) of cultured DRG (PNS) glia, DRG (PNS) neurons, hippocampal (CNS) neurons, and cortical (CNS) glia cells are shown. Immunoreactive bands representing SorCS2 isoforms are indicated by their molecular weight. Detection of actin served as loading control.

(H) WB of SorCS2 in HEK293 using polyclonal antibodies against the extracellular domain (αECD) or the propeptide (αPRO) of the receptor are shown.

(I) SorCS2 was immunoprecipitated from lysates of transfected cells treated with (+) or without (−) PNGase and visualized by WB (αECD).

(J) WB of lysates from SorCS2 transfected cells using αECD (left) or an antibody against the cytoplasmic tail (αCT) showing the presence of an additional band of 18 kDa (right).

(K) WB using αCT showing the presence 122 kDa form of SorCS2 in E14.5 dopaminergic neurons (7DIV) and brain homogenate from WT mice (left). The 122 kDa and 18 kDa bands are also present in DRG homogenates (right). No specific signals are observed in homogenate from SorCS2 KOs (−/−).

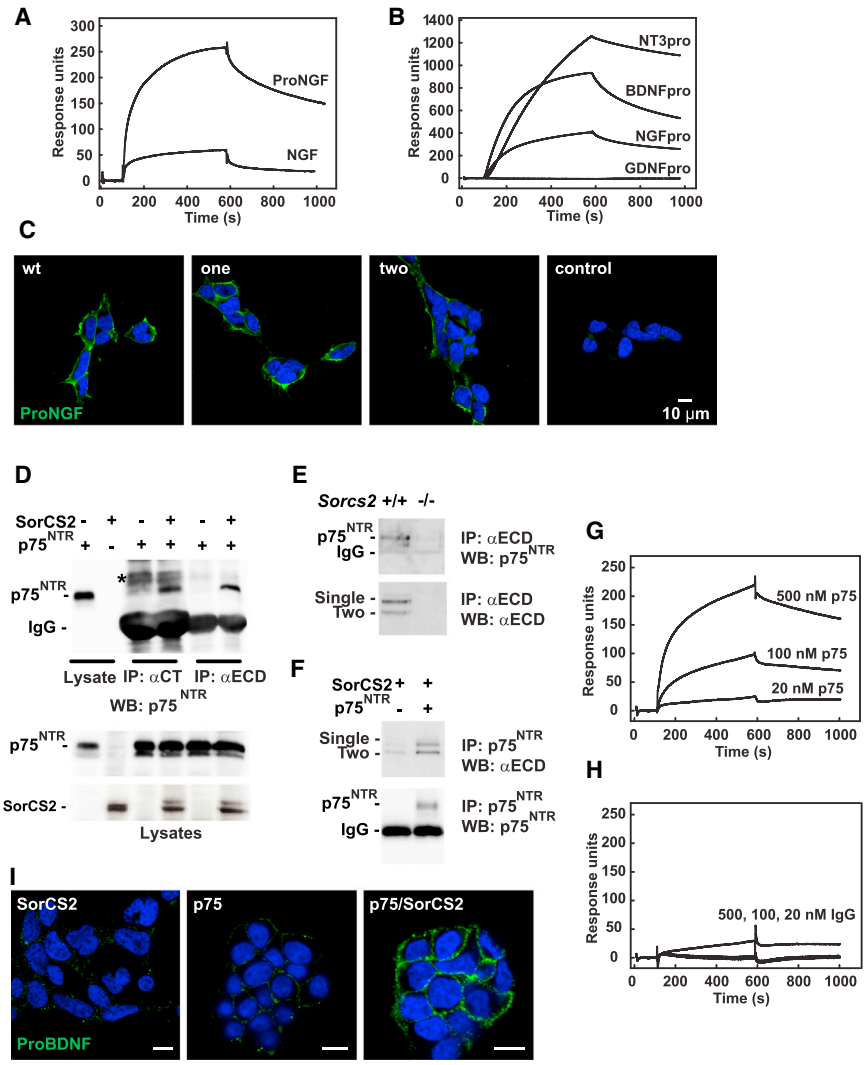

Figure 3. SorCS2 Isoforms Bind proNTs and p75^{NTR}

(A) SPR analysis demonstrates strong proNGF, but poor NGF (20 nM of each), binding to immobilized SorCS2.

(B) SorCS2 binds propeptides of NT3, BDNF, and NGF, but not of GDNF (20 nM of each propeptide).

(C) ProNGF (20 nM) binds to HEK293 cells transfected with the indicated SorCS2 variants. Mock transfected HEK293 cells were used as control.

(D) Coimmunoprecipitation (co-IP) of p75^{NTR} with SorCS2 in transfected HEK293 cells is shown. After crosslinking with a reducible crosslinker, SorCS2 was immunoprecipitated with αCT or αECD. Coprecipitated p75^{NTR} was depicted with WB analysis. Asterisk indicates two unspecific bands recognized by the p75^{NTR} antibody upon co-IP using αCT.

(E) Co-IP of endogenous p75^{NTR} with SorCS2 αECD from cerebellar homogenates of 8-week-old mice.

(F) The reverse experiment of (D) showing co-IP of both SorCS2 isoforms with p75^{NTR}.

(G and H) Concentration-dependent binding of Fc-tagged p75^{NTR} extracellular domain (G) but not of nonimmune rabbit IgG (H) to immobilized SorCS2 as shown with SPR.

(I) Binding of proBDNF (3 nM) to the surface of transfected HEK293 cells is greatly enhanced by the presence of both SorCS2 and p75^{NTR}. The level of p75^{NTR} expression was not altered by the presence of SorCS2 (data not shown).

extracellular domains is governed by the same intracellular sorting motifs (Figure S1G).

Taken together, we inferred that in CNS neurons SorCS2 exists as a single-chain receptor of 122 kDa whereas in PNS glia it is processed into a two-chain variant comprising a 104 kDa N-terminal domain that is noncovalently tethered to a smaller C-terminal fragment of 18 kDa (Figure 2E).

To study the dynamics of receptor processing in HEK293 cells, we metabolically labeled wild-type SorCS2 or the mutants in the presence of Brefeldin A to inhibit protein export from the endoplasmic reticulum. After labeling, the cells were washed and nascent receptor molecules chased for up to 22 hr (Figure 2F). As predicted, the propeptide of SorCS2-pro was liberated much slower and to a lesser extent than that of the wild-type receptor. In contrast, disrupting (SorCS2-one) or optimizing (SorCS2-two) the cleavage site at ^{1028}RKR^{1030} did not affect propeptide cleavage. Rather, it greatly shifted the balance between the one- and two-chain receptor isoforms and did so in a sequential manner. We concluded that propeptide cleavage is a prerequisite for subsequent two-chain processing of SorCS2.

Single- and Two-Chain SorCS2 Interact with proNTs and p75^{NTR}

Given that sortilin can bind proNGF, proBDNF, and proNT3 with high affinity, we exploited whether this also applies to SorCS2. The ectodomain of the receptor was immobilized on a biosensor chip and tested for proNT binding by surface plasmon resonance (SPR) analysis. ProNGF and proBDNF showed a robust interaction with SorCS2-sol corresponding to a K_d of ~5 nM, but mature NGF and BDNF bound only poorly (Figure 3A and data not shown). The proNT prodomains accounted for this interaction because the propeptides of proNGF, proBDNF, and proNT3, but not that of the glial-cell derived neurotrophic factor precursor (GDNFpro), bound SorCS2 avidly (Figure 3B). We next asked whether the SorCS2 isoforms can bind proNTs when exposed on the plasma membrane by incubating cells with 20 nM proNGF at 4°C for 120 min followed by anti-proNGF immunostaining. Because all three lines stained to a similar extent, we concluded that binding of proNTs is not restricted to one of the SorCS2 isoforms (Figure 3C).

Sortilin forms a complex with p75^{NTR} and we speculated SorCS2 might do the same (Nykjaer et al., 2004). Cells expressing wild-type SorCS2 and p75^{NTR} were subjected to coimmunoprecipitation using αECD or αCT antibodies followed by anti-p75^{NTR} immunoblotting (Figure 3D). SorCS2 robustly pulled

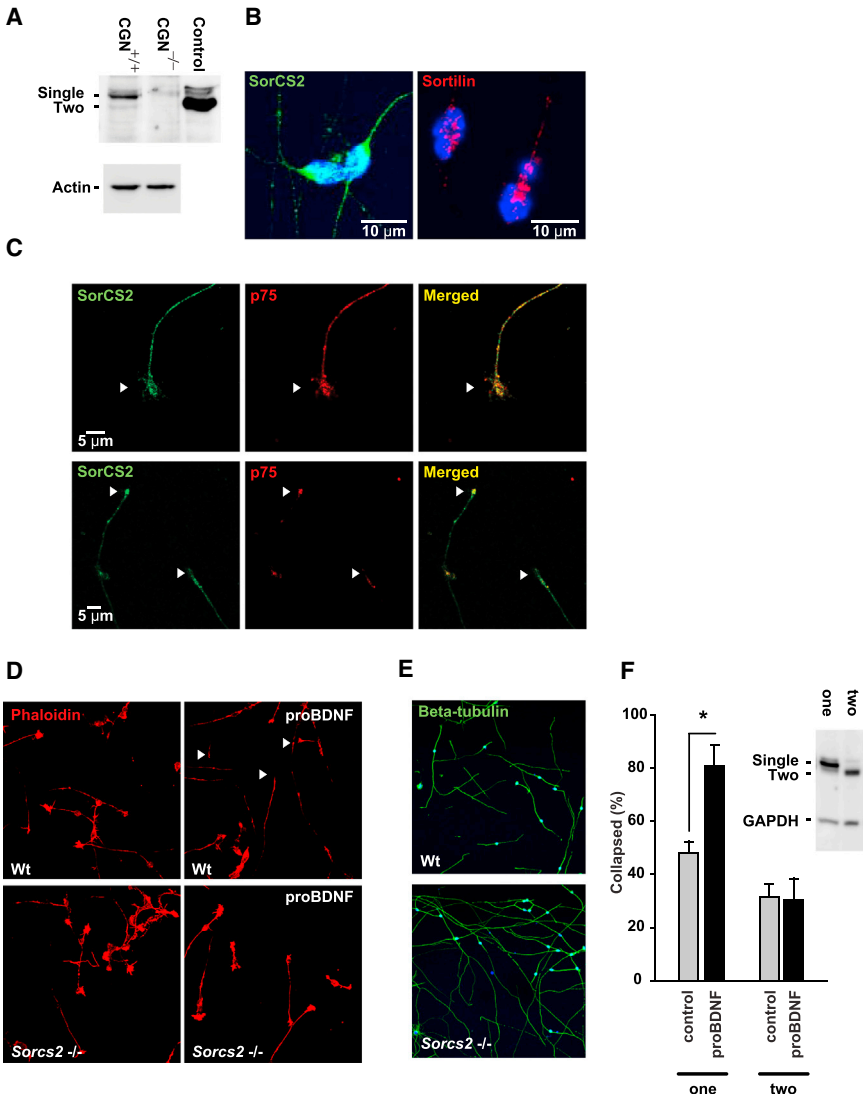

Figure 4. Single-Chain SorCS2 Is Required for Probdnf-Induced Growth Cone Collapse

(A) WB showing that SorCS2 is expressed as a single-chain isoform in cultured cerebellar granule neurons (CGN; 6 DIV) from WT mice (+/+). SorCS2 KO neurons (cf. Figure S3) are used as negative and transfected CHO cells as positive control. CHO cells produce mainly the two-chain form.

(B) Immunostaining of CGN for SorCS2 (green) and sortilin (red).

(C) SorCS2 (green) and $p75^{NTR}$ (red) in extending filopodia-rich projections (top) and collapsed growth cones (bottom) of CGN (6DIV) indicated by arrowheads.

(D) ProBDNF (10 ng/ml, 20 min) induces growth cone collapse in cultured CGN (3DIV) from WT mice but from not KO neurons. Growth cones were depicted with phaloidin staining (red). The experiment was performed four times with similar results. Arrowheads indicate collapsed growth cones.

(E) CGN derived from SorCS2 knockouts grow markedly longer neurites (depicted by staining for beta-tubulin; green).

(F) SorCS2-one, but not SorCS2-two, rescues proBDNF-induced growth cone collapse in transfected SorCS2 KO hippocampal neurons (3DIV). At least 50 transfected neurons were evaluated per coverslip on four independent coverslips per condition. The inset shows WB analysis of SorCS2-one and SorCS2-two in transfected KO neurons.

Error bars represent SEM. *$p < 0.05$. See also Figures S2 and S3.

down the highly glycosylated mature form of $p75^{NTR}$, which indicates complex formation at the cell surface. Importantly, $p75^{NTR}$ and SorCS2 also coprecipitated in cerebellum lysates of 8-week-old mice, signifying that complex formation can also occur when receptors are expressed at endogenous levels (Figure 3E). In the reverse situation, $p75^{NTR}$ coprecipitated both single- and two-chain SorCS2 from HEK293 cells transfected with $p75^{NTR}$ and wild-type SorCS2 (Figure 3F). Hence, two-chain processing does not affect the ability of $p75^{NTR}$ and SorCS2 to form heterodimers. In marked contrast to the interaction of $p75^{NTR}$ with sortilin (Nykjaer et al., 2004), proNTs did not strengthen the association with SorCS2 (data not shown). The interaction was direct and mediated by the extracellular receptor domain, because the $p75^{NTR}$ ectodomain fused to IgG-Fc bound immobilized SorCS2-sol with a K_d of ~10 nM. No binding was observed for IgG (Figures 3G and 3H).

Finally, we investigated whether SorCS2 and $p75^{NTR}$ cooperate in proNT binding. To this end, cells expressing SorCS2 and $p75^{NTR}$ separately or together were incubated with low concentrations (3 nM) of proNGF at 4°C followed by anti-proNGF immunostaining (Figure 3I). Binding to SorCS2 or $p75^{NTR}$ individually was barely detectable but surface labeling was greatly enhanced when the receptors were coexpressed. We inferred that coexpression of SorCS2 and $p75^{NTR}$ is required for efficient proNT binding.

Single-Chain SorCS2 Is Essential for proBDNF-Induced Growth Cone Collapse

A role for SorCS2 in axonal guidance was recently proposed because antireceptor antibodies attenuated growth cone retraction in cultured hippocampal neurons (Deinhardt et al., 2011). To extend these studies, we exploited growth cone morphology in neonatal cerebellar granule cells (CGN) because these cells express high levels of single-chain SorCS2 but not the 104 kDa two-chain variant (Figure 4A). As opposed to sortilin, which was mainly found in vesicular structures concentrated in the soma, SorCS2 was also abundant in axons and growth cones (Figure 4B). In the neurites, SorCS2 intensively colocalized with $p75^{NTR}$ in extending filopodia-rich projections and in collapsed growth cones, supporting a role in regulating growth cone decision (Figure 4C). To demonstrate a function for SorCS2 in axon retraction in vivo, we generated

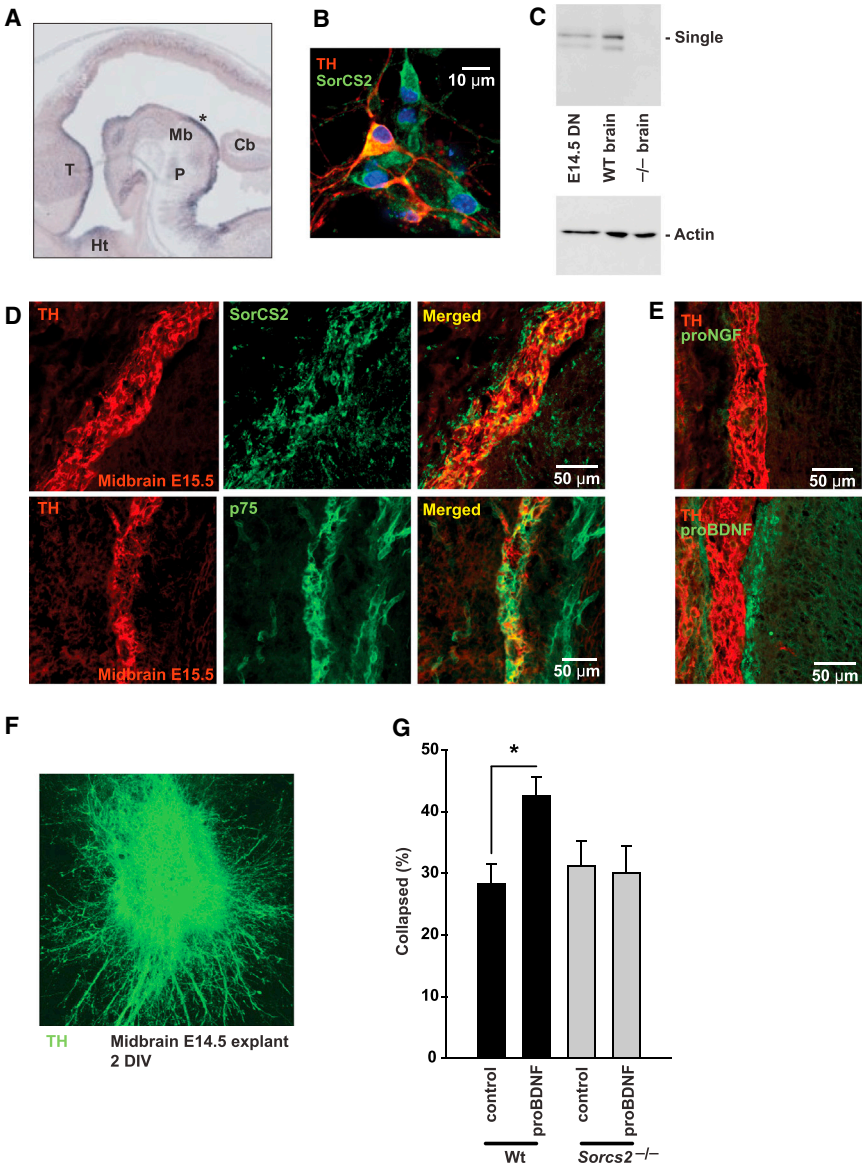

Figure 5. Growth Cone Collapse in the Developing Dopaminergic System Requires SorCS2

(A) In situ hybridization for *Sorcs2* on embryonic mouse tissue (E14.5) showing high expression in the midbrain area (Mb, asterisk). Cb, cerebellum; P, pons; T, thalamus; and Ht, hypothalamus.

(B and C) Expression of single-chain SorCS2 (green) in cultured embryonic TH^+ (red) neurons (E14.5DN, 7DIV) as analyzed by immunofluorescence (B) and WB using αECD (C).

(D) Double immunofluorescence staining demonstrates expression of SorCS2 (green, upper) and $p75^{NTR}$ (green, lower) in TH^+ cells (red) in sagittal sections of the murine E15.5 midbrain.

(E) Expression of proBDNF (green) but not proNGF in tissue surrounding the developing midbrain (stained for TH, red).

(F and G) SorCS2 mediates proBDNF-induced growth cone collapse. Midbrain E14.5 explants were cultured 2DIV prior to the addition of 10 ng/ml proBDNF for 20 min (F). The percentage of collapsed growth cones was subsequently scored by morphology (G). A minimum of 200 growth cones from at least 12 individual explants were evaluated for each condition (n = 4). Error bars represent SEM. *p < 0.05.

a SorCS2-deficient mouse and demonstrated with WB and immunofluorescence that expression of both receptor isoforms had been disrupted in CNS neurons (brain extracts, CGN cultures) and in PNS glia (sympathetic and dorsal root ganglia, respectively; Figures S2, 1K, and 4A). Knockout mice were viable, fertile, had a normal life span, and showed no histological abnormalities of the CNS (data not shown). First, we treated cultured CGNs from wild-type and knockout mice with proBDNF for 20 min to induce growth cone collapse in a $p75^{NTR}$-dependent manner (Koshimizu et al., 2009; Sun et al., 2012) and quantified retracted axons by labeling with the microtubule marker phalloidin (Figure 4D). Whereas control CGNs responded to proNT stimulation by a marked increase in growth cone collapse of ~57% (26.3% ± 1.76% versus 41.3% ± 2.36%, $p < 0.01$), *Sorcs2*$^{-/-}$ neurons failed to do so (28.7% ± 1.86% versus 33.7% ± 2.91%, $p = 0.22$). Likely, because of impaired sensitivity to endogenous proBDNF, knockout neurites were greatly extended compared to wild-types after 7 days in culture (Figure 4E). Of note, wild-type (WT) and knockout (KO) neurons showed identical localization of $p75^{NTR}$ in soma and neurites, suggesting that this effect was not accounted for by changes in the subcellular distribution of $p75^{NTR}$ (Figure S3). Remarkably, in SorCS2 knockout neurons proBDNF-induced growth cone collapse was rescued by expression of SorCS2-one, the isoform normally expressed in CNS neurons, but not by SorCS2-two, the predominant form in PNS (Figure 4F).

Single-Chain SorCS2 Is Critical in Shaping Mesolimbic Connectivity

To investigate whether SorCS2 may engage in establishing neuronal connectivity during development, we analyzed the embryonic expression pattern by in situ hybridization and immunohistochemistry at embryonic day 14.5 (E14.5) and E15.5, respectively (Figure S4). As opposed to the adult brain, SorCS2 was absent from the embryonic cerebellum, cortex, and dorsal hippocampus at E15.5 (Figure S4J). In contrast, mRNA transcripts were abundant not only in the mesencephalic flexure of the midbrain area (Figure 5A, asterisk), but also in the ventral hippocampus, the spinal cord, and in nonneuronal tissues such as heart and lung (Figure S4). Immunofluorescence microscopy

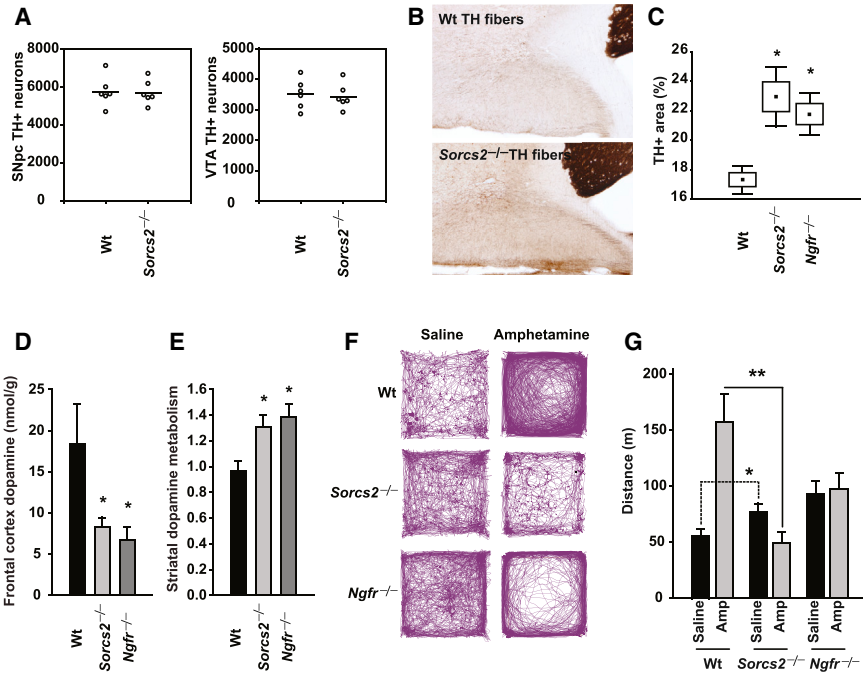

Figure 6. SorCS2 Is Critical for Establishing Dopaminergic Connectivity

(A) Stereological counts of TH$^+$ neurons in substantia nigra pars compacta (SNpc) and ventral tegmental area (VTA). Data for individual animals are given (8-month-old mice).

(B) Qualitative anatomical analysis of the dopaminergic system that revealed a marked increased density of TH fibers in the infralimbic cortex of SorCS2 KO animals (14 weeks old, six animals of each genotype) as shown with DAB immunohistochemistry on horizontal sections.

(C) The area covered by TH$^+$ DAB staining was quantified in the infralimbic cortex from WT mice, SorCS2 KO, and p75^{NTR} KO (14-week-old mice, four animals in each group). The results were evaluated using the Mann-Whitney U test.

(D and E) Reduced total dopamine levels and metabolism in the frontal cortex and striatum, respectively, of SorCS2 and p75^{NTR} KOs compared to WT as determined with high-performance liquid chromatography of 12-week-old WT and KOs, n = 8 per group. Dopamine metabolism was estimated as the dopamine levels divided by the sum of its metabolites.

(F) Track blots showing increased spontaneous motor activity in *Sorcs2*$^{-/-}$ and *Ngfr*$^{-/-}$ mice. While WT mice respond to amphetamine by hyperactivity, knockout animals are calmed by this treatment. Each image displays the trace (40 min) of one representative mouse for each condition.

(G) Quantification of hyperactivity as exemplified in(F) of ten WT, ten SorCS2-deficient, and nine p75^{NTR}-deficient mice (12–16 weeks old) treated with amphetamine (Amp) or saline (negative control).

Error bars represent SEM. $^{**}p < 0.01$, $^{*}p < 0.05$. See also Figure S5.

revealed enrichment of SorCS2 but not sortilin in tyrosine-hydroxylase positive (TH$^+$) neurons of the developing midbrain, which matures into the ventral tegmental area (VTA) and substantia nigra of the mature dopaminergic (DA) system (Figures 5D and S4K). To identify the isoform expressed in these neurons, we dissected out the embryonic midbrain and generated primary neuronal cultures. In accordance with the immunohistology, SorCS2 was prominent in TH-positive neurons with single-chain SorCS2 as the main isoform expressed (Figures 5B and 5C).

Given the heterodimerization of p75^{NTR} and SorCS2, we examined p75^{NTR} expression at day E15.5. Like SorCS2, p75^{NTR} was present in TH$^+$ neurons of the midbrain (Figure 5D), suggesting that they may cooperate in maturation of dopaminergic neurons. ProNGF was undetectable in this structure, but we observed abundant proBDNF expression in cells demarcating the DA neurons compatible with a function in axon guidance (Figure 5E). Hence, we investigated whether proBDNF can provoke DA growth cone collapse in E14.5 midbrain explants. Intriguingly, proBDNF induced a substantial collapse of TH$^+$ neurons in explants from wild-type animals whereas explants from SorCS2 knockouts were completely unresponsive (Figures 5F and 5G).

Defects in neuronal guidance during development would predict abnormal connectivity in the adult. Hence, we inspected the anatomy of the DA system in 12-week-old WT and *Sorcs2*$^{-/-}$ mice. TH-positive neurons were readily seen in all discrete dopaminergic cell groups of both genotypes (Figure S5 and data not shown). The number of neurons in the substantia nigra and VTA determined by stereologic quantification was also unaltered in the adult knockout mice, indicating that SorCS2 expression does not affect neuronal viability or migration of DA precursors (Figure 6A). In addition, the volume of the striatum as estimated using the principle of Cavalieri was similar for both genotypes ($1.00 \times 10^{-10} \pm 1.37 \times 10^{-9}$ μm^3 for WT and $0.95 \times 10^{-10} \pm 1.42 \times 10^{-9}$ μm^3 for KO, n = 8). Even so, we found that the frontal cortex, which receives DA input from the VTA, was strikingly hyperinnervated as shown with optical density image analysis (Figures 6B and 6C). TH-positive fibers of WT animals occupied 17% of the infralimbic area, a value that had increased to 23% in the SorCS2 KOs. Notably, mice lacking p75^{NTR} expression (*Ngfr*$^{-/-}$) exhibited a hyperinnervation that was identical to that observed in *Sorcs2*$^{-/-}$ mice (22% versus 23%; Figure 6C).

Sorcs2$^{-/-}$ Mice Exhibit ADHD-like Behavior

We next studied dopaminergic activity by measuring dopamine and its metabolites in the frontal cortex and striatum with high-performance liquid chromatography (Figures 6D and 6E). We found a marked reduction in dopamine levels of frontal cortex in SorCS2 and p75^{NTR} deficient animals ($p = 0.02$ and $p = 0.03$, respectively). In the striatum, the absolute dopamine concentrations were unaltered (data not shown) but dopamine metabolism was decreased in both KO models compared to WT mice. These changes possibly reflect compensatory adaptations to abnormal DA connectivity.

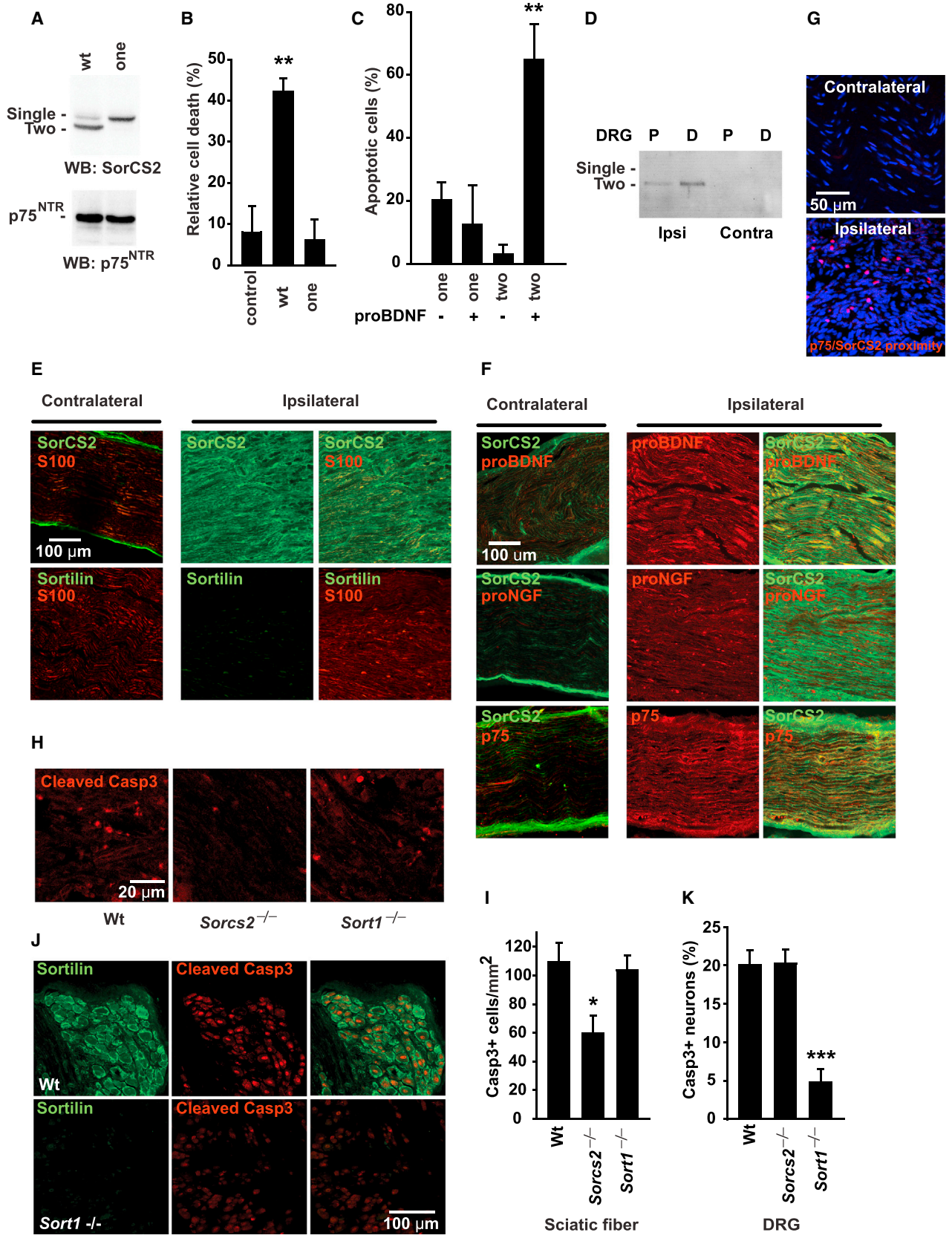

(legend on next page)

The combined effect of altered dopamine levels and metabolism and hyperinnervation of the frontal cortex would predict an abnormal response to psychostimulants. Thus, we subjected 12- to 16-week-old *Sorcs2*$^{-/-}$ mice to the open field test in the absence or presence of amphetamine treatment and measured their mobility during a 40 min trial period. Strikingly, vehicle-treated SorCS2 KOs were significantly more active than their WT controls ($p = 0.04$; Figures 6F and 6G). Furthermore, whereas amphetamine increased the distance traveled in WT animals from 56.2 ± 4.47 m to 158 ± 24.8 m ($p = 0.005$), we observed a paradoxical calming effect on *Sorcs2*$^{-/-}$ mice (from 76.7 ± 7.78 m to 49.7 ± 8.97 m, $p = 0.03$), a key symptom of attention deficit hyperactivity disorder (ADHD) in humans (Rappley, 2005). In agreement with the cooperativity of SorCS2 and p75^{NTR} in proBDNF binding, p75^{NTR}-deficient animals (*Ngfr*$^{-/-}$) were also hyperactive ($p = 0.02$) and showed a blunted response to amphetamine (Figures 6F and 6G).

Collectively, our data suggested that single-chain SorCS2 is critical for dopaminergic development by controlling growth cone retraction and target innervation.

Two-Chain SorCS2 Is Proapoptotic in Schwann Cells

Because sortilin is proapoptotic when coexpressed with p75^{NTR} (Nykjaer et al., 2004), we explored whether SorCS2 might also engage in apoptosis induction. To do so, RN22 Schwannoma cells that express endogenous p75^{NTR} were transfected with WT SorCS2 and cell death was scored after the addition of proNGF. As in the primary PNS glia cell cultures (cf. Figure 1G), SorCS2 was efficiently processed into its two-chain form in Schwannoma cells (Figure 7A). Treatment of the transfectants with proNGF for 72 hr increased cell death by more than 4-fold relative to mock transfected cells (Figure 7B). Intriguingly, whereas transfection with WT SorCS2 substantially increased Schwannoma cell death over that observed in control cells, SorCS2-one failed to do so. Similarly, in a rescue experiment using primary SorCS2 KO Schwann cells, transfection with two-chain, but not one-chain SorCS2, rendered the cells sensitive to proBDNF-induced apoptosis (Figure 7C). These observations indicate that two-chain processing is obligatory for SorCS2 to mediate cell death.

Two-Chain SorCS2 Mediates Schwann Cell Apoptosis In Vivo

SC apoptosis followed by demyelination is a prominent feature of peripheral nerve injury. Given the role of proNTs and p75^{NTR} in this process (Ferri and Bisby, 1999; Petratos et al., 2003; Soilu-Hänninen et al., 1999; Syroid et al., 2000), we explored whether SorCS2 might also be involved. With WB analysis, we first studied expression of single- and two-chain SorCS2 in ipsi- and contralateral nerve fibers after a sciatic nerve ligation of adult mice. On the injured side, there was a pronounced and selective increase in two-chain SorCS2 that was particularly prominent distal to the lesion site (Figures 7D and S8A). Whereas on the unlesioned side SorCS2 was confined to the epineurium, injury triggered a remarkable expression of the receptor in S100^{+} SCs in the distal stump. In contrast, sortilin was completely absent from these cells (Figure 7E). Injury also produced a striking coexpression of proBDNF, proNGF, and p75^{NTR} in the SorCS2-positive SC (Figure 7F), confirming previous reports that these proteins and their mRNAs are upregulated following a sciatic nerve lesion (Marcinkiewicz et al., 1998; Syroid et al., 2000; Tonra et al., 1998). We also observed a similar induction of SorCS2, p75^{NTR}, and proNTs in P2 mice analyzed 24 hr after the injury (Figure S6B and data not shown).

Taking this further, we investigated whether injury may stimulate SorCS2 and p75^{NTR} heterodimerization by use of in situ proximity ligation assay. This assay is based on hybridization of circular DNA probes coupled to antibodies. When probes are located less than 30 nm apart they will hybridize, and interacting proteins can be visualized with PCR using fluorescent-labeled nucleotides. Notably, we observed a red punctate staining on the injury side, reflecting juxtaposition of the receptors in the plasma membrane. No such labeling was seen in the contralateral uninjured nerve (Figure 7G).

Because all components of the extracellular apoptotic machinery (two-chain SorCS2, proNTs, and p75^{NTR}) were induced

Figure 7. SorCS2 and Sortilin Cooperate in Apoptosis Induction upon Peripheral Injury

(A) WB demonstrating expression of SorCS2-wt and SorCS2-one in transfected RN22 Schwannoma cells.

(B) Treatment with 100 ng/ml proNGF for 72 hr induces cell death in RN22 cells when transfected with SorCS2-wt (n = 4) but not with SorCS2-one as measured using quenched fluorescence-based assay for the number of live cells per well (n = 4).

(C) Treatment with 10 ng/ml proBDNF for 24 hr induced apoptosis in primary SCs from perinatal SorCS2 KO mice transfected with SorCS2-two but not SorCS2-one as determined by counting pycnotic and disintegrated nuclei (n = 4).

(D) Two-chain SorCS2 and p75^{NTR} are upregulated following sciatic nerve lesion (24 hr after surgery). Two-chain SorCS2 levels are increased both proximal (P) and distal (D) to the lesion (ipsilateral side) as determined with WB analysis (755% ± 243% and 2,018% ± 401%, respectively, compared to unlesioned nerve, n = 3, 50 μg tissue homogenate per lane; 12- to 16-week-old mice were used).

(E) Nerve injury increases SorCS2 (green, upper) but not sortilin (green, lower) expression in S100^{+} (red) SCs on the lesioned (ipsilateral) side (17 days after surgery). The distal side is shown.

(F) Immunofluorescence staining demonstrating colocalization of SorCS2 (green) with proBDNF (red, upper), proNGF (red, middle), and p75^{NTR} (red, bottom) distal to the lesion site.

(G) Proximity ligation assay demonstrating clusters of SorCS2 and p75^{NTR} located in proximity in injured but not in uninjured sciatic nerve fibers. Distal side is shown.

(H) Immunohistochemistry for activated caspase-3 in injured sciatic nerves distal from the site of injury in WT, *Sorcs2*$^{-/-}$, and *Sort1*$^{-/-}$ mice (17 days after injury). Data indicate reduced apoptosis in SorCS2-deficient animals.

(I) Quantification of caspase-3^{+} cells/mm^{2} distal from the injury as exemplified in (H). n = 3 animals in each group.

(J) Immunostaining for sortilin (green) and cleaved caspase-3 (red) in DRGs from WT (upper) and sortilin KO mice 17 days after injury.

(K) Quantification of cleaved caspase-3^{+} DRG neurons from three WT, *Sorcs2*$^{-/-}$, and *Sort1*$^{-/-}$ mice, respectively.

Error bars represent SEM. ***$p < 0.001$, **$p < 0.01$, *$p < 0.05$. See also Figures S6 and S7.

after sciatic nerve injury, we compared caspase-3 activation ($Casp3^+$) and DNA fragmentation (TUNEL) in adult WT and $Sorcs2^{-/-}$ animals 17 days after surgery. The neuronal composition of the DRG, the morphology of the sciatic nerve, number of SCs, and peripheral innervation as determined by nociception, tactile sensation, and motor function were identical in naive WT and SorCS2 KO animals prior to the injury (Figure S7). Notably, SC apoptosis was substantially reduced distal to the lesion in the SorCS2-deficient mice as shown by a reduction in $Casp3^+$ and TUNEL-positive cells of ~46% and ~51%, respectively (Figures 7H and 7I and S8C and S8D). For comparison, mice devoid in sortilin expression ($Sort1^{-/-}$) showed no protection against caspase-3 activation (Figures 7H and 7I). In P2 animals, the number of TUNEL-positive cells was diminished by 34% in the SorCS2 KOs 24 hr after injury, demonstrating the importance of the receptor for SC apoptosis in the neonatal period (Figure S6E).

Neuronal loss is also a key feature of nerve injury. We therefore stained DRGs for Casp3 activation 17 days after lesioning. As opposed to SorCS2, which was confined to satellite cells (cf. Figure 1E), sortilin was present exclusively in neurons (Figure 7J). In marked contrast to the protective effect of SorCS2-deficiency on SC apoptosis, it did not safeguard the corresponding neurons from caspase-3 activation (Figure 7K). Conversely, sortilin-deficiency did not affect SC apoptosis, although it reduced activated $Casp3^+$ neurons by ~80% (Figures 7I and 7K). The data suggest that two-chain SorCS2 and sortilin subserve similar apoptosis-inducing activities but do so in distinct cell types. Whereas SorCS2 operates in Schwann cells, sortilin induces apoptosis in the corresponding neurons.

DISCUSSION

Sculpturing the neuronal network and fine-tuning of synaptic contacts rely on an intricate balance between guidance cues, growth cone morphogens, and trophic and apoptotic signals regulating neuron and glia cell fate. The mechanisms that govern these activities are incompletely understood but neurotrophins have long been considered critical. According to the neurotrophic factor hypothesis, depriving neurons of their trophic support leads to synaptic weakening and/or neuronal degeneration. However, signals elicited by proNTs may augment these activities or may even override signals that are simultaneously provided by NTs (Nykjaer and Willnow, 2012; Song et al., 2010). These observations imply that proteolytic processing of proNTs to their mature forms, by switching receptor specificity, can elicit opposing signaling events to regulate cell fate. Our findings add another level of complexity by which trophic and apoptotic signaling can be regulated. First, we identify SorCS2 as a proNT receptor capable of inducing both growth cone collapse and apoptosis in vivo. Second, we show that cell fate decision is not limited to proteolytic processing of the ligand but also depends on receptor processing. While single-chain SorCS2 regulates axon guidance of developing midbrain dopaminergic processes, two-chain processing in PNS glia transforms the receptor into a transducer of apoptotic signals. To our knowledge, this is the first example to demonstrate that cell type-specific receptor processing may regulate two distinct biological functions.

During development, single-chain SorCS2 is abundant in dopaminergic precursors of the developing midbrain. Several lines of evidence underpin the biological relevance of SorCS2 for growth cone collapse during development. First, proBDNF potently induced axonal retraction of TH^+ neurons in E14.5 midbrain explants from WT but not $Sorcs2^{-/-}$ explants. Second, transfection of KO neurons with single-, but not two-chain, rescued the proBDNF sensitivity. In adult $Sorcs2^{-/-}$ mice, DA functionality of the mesolimbic system was severely afflicted despite an unaltered number of midbrain dopaminergic neurons. Conceivable, this is the consequence of the faulty prefrontal innervation rather than acute effects on synaptic transmission because studies have demonstrated that SorCS2 expression in the VTA is limited to the period during which dopaminergic neurons differentiate and axonal processes reach their targets (Hermey et al., 2001; Rezgaoui et al., 2001).

A number of studies have reported that patients with ADHD commonly exhibit miswiring of the prefrontal cortex and striatum accompanied by altered dopaminergic function (Liston et al., 2011). It is noteworthy that the majority of ADHD risk genes identified in genome-wide associations studies (GWAS) are associated with regulation of neurite outgrowth (Poelmans et al., 2011). Also, results of recent studies suggested that SNPs in the coding regions of proNT3, proNGF, and proBDNF are genetically linked to ADHD. In particular, SNPs in their prodomains that harbor the SorCS2 binding motif were uncovered in several independent cohorts (Conner et al., 2008; Ribasés et al., 2008; Syed et al., 2007). Perhaps most strikingly, a recent genome-wide association study examining 500.000 SNPs identified a polymorphism in the *SORCS2* locus that was strongly linked to risk of ADHD (Lesch et al., 2008).

As opposed to CNS neurons that express single-chain SorCS2, PNS glia produce the two-chain variant of the receptor. Studies in Schwannoma cells and primary SCs established that the apoptotic response to proNTs was specific to two-chain SorCS2. Injury to the PNS often causes permanent neurological deficits due to disruption of the myelin-axonal unit, resulting in a poor capacity of the neurons to regenerate (Chen et al., 2007). We found that nerve injury was accompanied by a selective upregulation of two-chain SorCS2 in the Schwann cells. The substantial reduction in SC apoptosis in lesioned $Sorcs2^{-/-}$ mice clearly emphasizes the relevance of two-chain processing in vivo.

Surprisingly, despite the disparate functions of single- and two-chain SorCS2 in CNS neurons and PNS glia, both activities require complex formation with $p75^{NTR}$ and proNTs. Thus, single-chain and two-chain SorCS2 can physically interact with $p75^{NTR}$ and cooperate in proNT binding. Single-chain SorCS2 and $p75^{NTR}$ receptors colocalize in axonal filopodia and are expressed in DA neurons of the ventral midbrain flexure. ProBDNF is in the vicinity because it is abundant in the demarcating tissue in which axons project. Furthermore, SorCS2 and $p75^{NTR}$ KO mice had reduced DA levels and metabolism in the frontal cortex and striatum, respectively, were hyperinnervated with TH-positive fibers, hyperactive, and exhibited a paradoxical calming response to amphetamine. Importantly, these data are supported by recent studies reporting that $p75^{NTR}$ is obligate for

cultured hippocampal neurons to respond to proNT by growth cone retraction (Deinhardt et al., 2011; Sun et al., 2012). Finally, following peripheral nerve injury, expression of two-chain SorCS2, but not the single-chain form, was upregulated. In addition, $p75^{NTR}$, proBDNF, and proNGF were strongly induced and proximity ligation assay showed clustering of SorCS2 and $p75^{NTR}$ in SCs. The 46% reduction in lesion-induced SC apoptosis observed for *Sorcs2*$^{-/-}$ mice matches values previously reported for $p75^{NTR}$-deficient mice or mice treated with polyclonal antibodies targeting proNGF/NGF (Petratos et al., 2003; Syroid et al., 2000). The combined observations support that SorCS2 and $p75^{NTR}$ jointly regulate SC apoptosis in lesioned nerves of the PNS.

Like sortilin, SorCS2 is produced as a proreceptor containing a sequence of 69 amino acids after the signal peptide. In sortilin, the propetide prevents premature ligand binding in the biosynthetic pathway. Once exiting the late trans-Golgi compartment, the propetide is liberated by furin-mediated cleavage, conditioning the receptor for full functional activity (Munck Petersen et al., 1999). The role of propeptide in SorCS2 is so far unknown but it is plausible that it functions in a similar manner to shield the ligand-binding site. In support of a regulatory function, two-chain processing did not take place until the propeptide had been released. In another scenario, the propetide might facilitate receptor folding and secure expedited transport of SorCS2 through the biosynthetic pathway. Studies are currently ongoing to address these possibilities.

The enzyme(s) and cellular compartment(s) involved in the two-chain cleavage of SorCS2 are currently unknown. However, once processed, the two chains remain associated by a noncovalent interaction. SorCS2 belongs to the group of leucine-rich repeat transmembrane proteins, members of which many are involved in axon guidance, including Slit, Slitrk, the Nogo receptors, and TrkA, -B, and -C. In these proteins, the leucine-rich repeat domains create a versatile structural framework for protein-protein interactions. The repeats are formed by two β strands connected by a loop region of variable sequence and structure and are arranged in a curved horseshoe-like structure. Globular ligands fit into this structure but their access is permitted or prohibited by the relative position of the β strands (de Wit et al., 2011). Two-chain conversion occurs in the leucine-rich repeat domain of SorCS2 and secondary structure analysis using the Jpred3 algorithm (Cole et al., 2008) predicts that the cleavage site is located in a loop between the two β strands (data not shown). Cleavage at this site would likely add additional degrees of freedom to the tertiary structure of the domain allowing or preventing access of new ligands or yet unknown coreceptors. This could provide the molecular basis for the different biological functions of single- to two-chain conversion of SorCS2.

In conclusion, we have found that SorCS2 exists in two isoforms with distinct activities. The single-chain from is expressed in CNS neurons and is required for growth cone collapse of dopaminergic neurons, but in PNS glia, proteolytic processing converts the receptor into a transducer of apoptosis signals. To the best of our knowledge, this is the first example to demonstrate that a receptor, taking advantage of the same ligand and same coreceptor, can exhibit disparate functions depending on its proteolytic processing. Our findings add a new dimension to our understanding of the mechanisms that govern receptor multifunctionality.

EXPERIMENTAL PROCEDURES

Targeting of the Murine *Sorcs2* Locus

Exon 15 of murine SorCS2 was disrupted by insertion of a cassette comprising an internal ribosomal entry-site followed by the reporter gene LacZ and a Neo-resistance gene for positive selection. The targeting vector was constructed by flanking the cassette with a 1.2 kb (short arm) and 8.0 kb (long arm) fragment of the murine SorCS2 DNA. The short 1.2 kb fragment was generated by PCR and inserted into the unique NotI site and the long arm was introduced into the targeting vector in the unique XhoI site. Two copies of the herpes simplex virus thymidine kinase gene were included 5′ to the short arm and used as for negative selection. Electroporation of embryonic stem cell line ICp4 and derivation of germline chimeras were performed according to standard procedures. The disrupted allele was confirmed with Southern blotting of HindIII digested genomic DNA using a 900 b hybridization probe, giving a WT allele of ~10 kb and disrupted allele of 6 kb. In the present experiments, all mice had been backcrosses for ten generations into C57BL/6J. All experiments were approved by the Danish Animal Experiments Inspectorate under the Ministry of Justice.

Antibodies

The purified soluble extracellular domain of human SorCS2 (sSorCS2) was used to generate rabbit polyclonal anti-SorCS2 antibodies (αECD) as well as mouse monoclonal antibodies (Mikkel R. Holst and A.N., unpublished data). The last 28 amino acids of murine SorCS2 cytoplasmic tail were expressed as a GST fusion protein as described above and used for generation of rabbit polyclonal anti-SorCS2 antibodies (αCT). Antibodies recognizing GST were subsequently depleted on a column coupled with GST. The specificity of αCT was subsequently confirmed using lysates of HEK293 cells expressing a SorCS2 variant lacking its cytoplasmic tail as negative control. Rabbit polyclonal antibodies recognizing the propeptide of SorCS2 (αPRO) were generated in a similar manner. See the Supplemental Experimental Procedures for additional information on the use of antibodies. The performance of all tested antibodies was shared on the public database http://www.pabmabs.com.

Sciatic Nerve Ligation

Adult male mice (12 to 16 weeks old) were anesthetized with ketamine/xylazine and the left sciatic nerve was double ligated at midthigh level. After 17 days, the animals were killed and nerve fibers were isolated from the ipsilateral and contralateral sides. After fixation in 4% paraformaldehyde with cryoprotection in 30% sucrose, the nerve fibers were embedded in Tissue-Tek O.C.T. compound, snap-frozen on dry ice, and cryosectioned at 14 μm. Every fifth section was scored for cleaved caspase-3 or TUNEL-positive cells per square millimeter nerve at a distance of 1 mm from the site of injury by an investigator blinded to the identity of the samples. Similarly, cleaved caspase-3-positive neurons were scored in the DRG L4. Ligation on P2 mice was performed as described elsewhere (Syroid et al., 2000). Briefly, postnatal day 2 mice were rendered unconscious under ice-induced hypothermia and the left sciatic nerve was exposed and ligated (two knots) with 8.0 suture. Lidocaine was applied to the wound/nerve, and the skin was closed using 8.0 surgical sutures. The pups were allowed to warm up, and when fully conscious were returned to their mothers. Twenty-four hr after axotomy, pups were decapitated, and the proximal and distal segments of the ligated left sciatic nerve were removed, along with the intact right sciatic nerve as control.

Stereology

Six SorCS2 KO and six WT brains from 8-month-old mice were perfusion-fixed with phosphate-buffered 4% formaldehyde through the left ventricle for 5 min and postfixed overnight in the same fixative. Following sucrose treatment, the brains were frozen in isopentan and cut into 60-μm-thick sections on a cryostat. Every third section was sampled systematically and stained with primary rabbit-anti-TH (Pel-Freez, P40101) 1:1,000, secondary goat-anti-rabbit (DAKO, P0448) 1:200, and depicted by 3,3′-diaminobenzidine (Sigma-Aldrich,

D05637). The total number of TH^+ neurons was estimated by the optical fractionator with varying height sampling fraction (Dorph-Petersen and Lewis, 2011) using an Olympus BX 50 light microscope equipped with a Prior motorized stage, a Heidenhain microcator, Olympus UPlanSApo 60x oil lens (NA = 1.35), and an Olympus DP70 digital camera controlled by newCAST (Visiopharm) software. The step lengths in x- and y-directions were 60 μm, the area of the two-dimensional unbiased counting frame was 1,615 μm, and the disector height was 10 μm. The TH^+ neurons were counted in substantia nigra pars centralis and VTA in one side of the brain chosen at random. The coefficients of error of the two number estimates were both ~9% (Gundersen et al., 1999).

Eight SorCS2 and Eight WT mice brains (9 weeks old) were perfusion fixed as above and cut on a Vibratome 3000 into 60-μm thick sections with every third section sampled systematically. Staining against TH was performed as above and sections were depicted on the same microscope using an Olympus UPlanApo 4x lens (NA = 0.16). The Cavalieri estimator and the two-dimensional nucleator with five test rays in the newCAST software were used to estimate the volume of the left or right of striatum chosen at random.

Behavior

Amphetamine (10 mg/kg) or saline was administered intraperitoneally to WT, *Sorcs2*$^{-/-}$, or *Ngfr*$^{-/-}$ male C57BL/6J mice (12–16 weeks old), and the mice were tested immediately after administration (always during the light cycle) for amphetamine-induced hyperactivity in an open field test consisting of a (40 × 40 × 35 cm) clear Plexiglas arena. Mice were placed in the corner of the arena and their activity was recorded over a 40 min session and analyzed using the Any-maze tracking system. Von Frey and hot plate tests were performed as described elsewhere (Vaegter et al., 2011). Motor coordination in WT and *Sorcs2*$^{-/-}$ mice was investigated using a rotarod (Model LE 8200, Panlab). The speed accelerated from 4 to 40 rpm over a 5 min period (linear increase). Mice were brought to the test room 1 hr prior to the test. Mice were placed on a rotating drum, and the time they remained on the rotarod was registered automatically. The mice were tested over 2 consecutive days, where the first day was a training day, and on the second day, the mice were first put through a training session then the time on the rotarod was recorded.

Statistics

Data are presented as mean values ± SEM. Unless mentioned otherwise, significance was evaluated using a two-tailed t test.

SUPPLEMENTAL INFORMATION

Supplemental Information includes Supplemental Experimental Procedures and seven figures and can be found with this article online at http://dx.doi.org/10.1016/j.neuron.2014.04.022.

ACKNOWLEDGMENTS

This study was funded by the Lundbeck Foundation (to A.N. and C.M.P.), Danish Medical Research Council (to S.G.), the Deutsche Forschungsgemeinschaft (to T.E.W.), and EuReGene (FP6 005085 to A.N., T.E.W., and G.E.). We thank Dariusz Orlowski, PhD, for quantitative image analysis, Pernille Jansen and Mette Richner (Aarhus University) and Giulia Ronchi and Stefano Geuna (University of Turin) for providing data to the characterization of the peripheral nervous system, and Anja Aagaard, Benedicte Vestergaard, and Trine W. Mikkelsen for excellent technical assistance.

Accepted: April 8, 2014
Published: June 4, 2014

REFERENCES

Arancio, O., and Chao, M.V. (2007). Neurotrophins, synaptic plasticity and dementia. Curr. Opin. Neurobiol. *17*, 325–330.

Beattie, M.S., Harrington, A.W., Lee, R., Kim, J.Y., Boyce, S.L., Longo, F.M., Bresnahan, J.C., Hempstead, B.L., and Yoon, S.O. (2002). ProNGF induces p75-mediated death of oligodendrocytes following spinal cord injury. Neuron *36*, 375–386.

Chao, M.V. (2003). Neurotrophins and their receptors: a convergence point for many signalling pathways. Nat. Rev. Neurosci. *4*, 299–309.

Chen, Z.L., Yu, W.M., and Strickland, S. (2007). Peripheral regeneration. Annu. Rev. Neurosci. *30*, 209–233.

Cole, C., Barber, J.D., and Barton, G.J. (2008). The Jpred 3 secondary structure prediction server. Nucleic Acids Res. *36* (Web Server issue), W197–W201.

Conner, A.C., Kissling, C., Hodges, E., Hünnerkopf, R., Clement, R.M., Dudley, E., Freitag, C.M., Rösler, M., Retz, W., and Thome, J. (2008). Neurotrophic factor-related gene polymorphisms and adult attention deficit hyperactivity disorder (ADHD) score in a high-risk male population. Am. J. Med. Genet. B. Neuropsychiatr. Genet. *147B*, 1476–1480.

de Wit, J., Hong, W., Luo, L., and Ghosh, A. (2011). Role of leucine-rich repeat proteins in the development and function of neural circuits. Annu. Rev. Cell Dev. Biol. *27*, 697–729.

Deinhardt, K., Kim, T., Spellman, D.S., Mains, R.E., Eipper, B.A., Neubert, T.A., Chao, M.V., and Hempstead, B.L. (2011). Neuronal growth cone retraction relies on proneurotrophin receptor signaling through Rac. Sci. Signal. *4*, ra82.

Dorph-Petersen, K.A., and Lewis, D.A. (2011). Stereological approaches to identifying neuropathology in psychosis. Biol. Psychiatry *69*, 113–126.

Ferri, C.C., and Bisby, M.A. (1999). Improved survival of injured sciatic nerve Schwann cells in mice lacking the p75 receptor. Neurosci. Lett. *272*, 191–194.

Gundersen, H.J., Jensen, E.B., Kiêu, K., and Nielsen, J. (1999). The efficiency of systematic sampling in stereology—reconsidered. J. Microsc. *193*, 199–211.

Hermey, G., Schaller, H.C., and Hermans-Borgmeyer, I. (2001). Transient expression of SorCS in developing telencephalic and mesencephalic structures of the mouse. Neuroreport *12*, 29–32.

Huang, E.J., and Reichardt, L.F. (2003). Trk receptors: roles in neuronal signal transduction. Annu. Rev. Biochem. *72*, 609–642.

Ibáñez, C.F., and Simi, A. (2012). p75 neurotrophin receptor signaling in nervous system injury and degeneration: paradox and opportunity. Trends Neurosci. *35*, 431–440.

Jansen, P., Giehl, K., Nyengaard, J.R., Teng, K., Lioubinski, O., Sjoegaard, S.S., Breiderhoff, T., Gotthardt, M., Lin, F., Eilers, A., et al. (2007). Roles for the pro-neurotrophin receptor sortilin in neuronal development, aging and brain injury. Nat. Neurosci. *10*, 1449–1457.

Koshimizu, H., Kiyosue, K., Hara, T., Hazama, S., Suzuki, S., Uegaki, K., Nagappan, G., Zaitsev, E., Hirokawa, T., Tatsu, Y., et al. (2009). Multiple functions of precursor BDNF to CNS neurons: negative regulation of neurite growth, spine formation and cell survival. Mol. Brain *2*, 27.

Lee, R., Kermani, P., Teng, K.K., and Hempstead, B.L. (2001). Regulation of cell survival by secreted proneurotrophins. Science *294*, 1945–1948.

Lesch, K.P., Timmesfeld, N., Renner, T.J., Halperin, R., Röser, C., Nguyen, T.T., Craig, D.W., Romanos, J., Heine, M., Meyer, J., et al. (2008). Molecular genetics of adult ADHD: converging evidence from genome-wide association and extended pedigree linkage studies. J. Neural Transm. *115*, 1573–1585.

Liston, C., Malter Cohen, M., Teslovich, T., Levenson, D., and Casey, B.J. (2011). Atypical prefrontal connectivity in attention-deficit/hyperactivity disorder: pathway to disease or pathological end point? Biol. Psychiatry *69*, 1168–1177.

Marcinkiewicz, M., Savaria, D., and Marcinkiewicz, J. (1998). The pro-protein convertase PC1 is induced in the transected sciatic nerve and is present in cultured Schwann cells: comparison with PC5, furin and PC7, implication in pro-BDNF processing. Brain Res. Mol. Brain Res. *59*, 229–246.

Munck Petersen, C., Nielsen, M.S., Jacobsen, C., Tauris, J., Jacobsen, L., Gliemann, J., Moestrup, S.K., and Madsen, P. (1999). Propeptide cleavage conditions sortilin/neurotensin receptor-3 for ligand binding. EMBO J. *18*, 595–604.

Nykjaer, A., and Willnow, T.E. (2012). Sortilin: a receptor to regulate neuronal viability and function. Trends Neurosci. *35*, 261–270.

Nykjaer, A., Lee, R., Teng, K.K., Jansen, P., Madsen, P., Nielsen, M.S., Jacobsen, C., Kliemannel, M., Schwarz, E., Willnow, T.E., et al. (2004). Sortilin is essential for proNGF-induced neuronal cell death. Nature *427*, 843–848.

Nykjaer, A., Willnow, T.E., and Petersen, C.M. (2005). p75NTR—live or let die. Curr. Opin. Neurobiol. *15*, 49–57.

Petratos, S., Butzkueven, H., Shipham, K., Cooper, H., Bucci, T., Reid, K., Lopes, E., Emery, B., Cheema, S.S., and Kilpatrick, T.J. (2003). Schwann cell apoptosis in the postnatal axotomized sciatic nerve is mediated via NGF through the low-affinity neurotrophin receptor. J. Neuropathol. Exp. Neurol. *62*, 398–411.

Poelmans, G., Pauls, D.L., Buitelaar, J.K., and Franke, B. (2011). Integrated genome-wide association study findings: identification of a neurodevelopmental network for attention deficit hyperactivity disorder. Am. J. Psychiatry *168*, 365–377.

Quistgaard, E.M., Madsen, P., Grøftehauge, M.K., Nissen, P., Petersen, C.M., and Thirup, S.S. (2009). Ligands bind to Sortilin in the tunnel of a ten-bladed beta-propeller domain. Nat. Struct. Mol. Biol. *16*, 96–98.

Rappley, M.D. (2005). Clinical practice. Attention deficit-hyperactivity disorder. N. Engl. J. Med. *352*, 165–173.

Rezgaoui, M., Hermey, G., Riedel, I.B., Hampe, W., Schaller, H.C., and Hermans-Borgmeyer, I. (2001). Identification of SorCS2, a novel member of the VPS10 domain containing receptor family, prominently expressed in the developing mouse brain. Mech. Dev. *100*, 335–338.

Ribasés, M., Hervás, A., Ramos-Quiroga, J.A., Bosch, R., Bielsa, A., Gastaminza, X., Fernández-Anguiano, M., Nogueira, M., Gómez-Barros, N., Valero, S., et al. (2008). Association study of 10 genes encoding neurotrophic factors and their receptors in adult and child attention-deficit/hyperactivity disorder. Biol. Psychiatry *63*, 935–945.

Rösch, H., Schweigreiter, R., Bonhoeffer, T., Barde, Y.A., and Korte, M. (2005). The neurotrophin receptor p75NTR modulates long-term depression and regulates the expression of AMPA receptor subunits in the hippocampus. Proc. Natl. Acad. Sci. USA *102*, 7362–7367.

Skeldal, S., Matusica, D., Nykjaer, A., and Coulson, E.J. (2011). Proteolytic processing of the p75 neurotrophin receptor: A prerequisite for signalling?: Neuronal life, growth and death signalling are crucially regulated by intra-membrane proteolysis and trafficking of p75(NTR). Bioessays. *33*, 614–625.

Soilu-Hänninen, M., Ekert, P., Bucci, T., Syroid, D., Bartlett, P.F., and Kilpatrick, T.J. (1999). Nerve growth factor signaling through p75 induces apoptosis in Schwann cells via a Bcl-2-independent pathway. J. Neurosci. *19*, 4828–4838.

Song, W., Volosin, M., Cragnolini, A.B., Hempstead, B.L., and Friedman, W.J. (2010). ProNGF induces PTEN via p75NTR to suppress Trk-mediated survival signaling in brain neurons. J. Neurosci. *30*, 15608–15615.

Sun, Y., Lim, Y., Li, F., Liu, S., Lu, J.J., Haberberger, R., Zhong, J.H., and Zhou, X.F. (2012). ProBDNF collapses neurite outgrowth of primary neurons by activating RhoA. PLoS ONE *7*, e35883.

Syed, Z., Dudbridge, F., and Kent, L. (2007). An investigation of the neurotrophic factor genes GDNF, NGF, and NT3 in susceptibility to ADHD. Am. J. Med. Genet. B. Neuropsychiatr. Genet. *144B*, 375–378.

Syroid, D.E., Maycox, P.J., Soilu-Hänninen, M., Petratos, S., Bucci, T., Burrola, P., Murray, S., Cheema, S., Lee, K.F., Lemke, G., and Kilpatrick, T.J. (2000). Induction of postnatal schwann cell death by the low-affinity neurotrophin receptor in vitro and after axotomy. J. Neurosci. *20*, 5741–5747.

Tauris, J., Gustafsen, C., Christensen, E.I., Jansen, P., Nykjaer, A., Nyengaard, J.R., Teng, K.K., Schwarz, E., Ovesen, T., Madsen, P., and Petersen, C.M. (2011). Proneurotrophin-3 may induce Sortilin-dependent death in inner ear neurons. Eur. J. Neurosci. *33*, 622–631.

Teng, H.K., Teng, K.K., Lee, R., Wright, S., Tevar, S., Almeida, R.D., Kermani, P., Torkin, R., Chen, Z.Y., Lee, F.S., et al. (2005). ProBDNF induces neuronal apoptosis via activation of a receptor complex of p75NTR and sortilin. J. Neurosci. *25*, 5455–5463.

Tonra, J.R., Curtis, R., Wong, V., Cliffer, K.D., Park, J.S., Timmes, A., Nguyen, T., Lindsay, R.M., Acheson, A., and DiStefano, P.S. (1998). Axotomy upregulates the anterograde transport and expression of brain-derived neurotrophic factor by sensory neurons. J. Neurosci. *18*, 4374–4383.

Vaegter, C.B., Jansen, P., Fjorback, A.W., Glerup, S., Skeldal, S., Kjolby, M., Richner, M., Erdmann, B., Nyengaard, J.R., Tessarollo, L., et al. (2011). Sortilin associates with Trk receptors to enhance anterograde transport and neurotrophin signaling. Nat. Neurosci. *14*, 54–61.

Woo, N.H., Teng, H.K., Siao, C.J., Chiaruttini, C., Pang, P.T., Milner, T.A., Hempstead, B.L., and Lu, B. (2005). Activation of p75NTR by proBDNF facilitates hippocampal long-term depression. Nat. Neurosci. *8*, 1069–1077.

Yano, H., Torkin, R., Martin, L.A., Chao, M.V., and Teng, K.K. (2009). Proneurotrophin-3 is a neuronal apoptotic ligand: evidence for retrograde-directed cell killing. J. Neurosci. *29*, 14790–14802.